Theoretical modeling of the ligand-tuning effect over the transition temperature in four-coordinated Fe^{II} molecules

Jordi Cirera[1],* and Eliseo Ruiz[1]

[1] Departament de Química Inorgànica and Institut de Recerca de Química Teòrica i Computacional, Universitat de Barcelona, Diagonal 645, 08028 Barcelona, Spain

Email corresponding authors: jordi.cirera@qi.ub.es, eliseo.ruiz@qi.ub.es

Keywords: Spin-Crossover, Density Functional Theory, Transition Metal Complexes, Tolman Cone Angle, Transition Temperature.

Abstract

Spin-crossover molecules are systems of great interests due to their behavior as molecular level switches, which makes them promising candidates for nanoscale memory devices, among other applications. In this paper we report a computational study for the calculation of the transition temperature ($T_{1/2}$), a key physical quantity in the characterization of spin-crossover systems, for the family of tetracoordinated Fe^{II} transition metal complexes of generic formula $[PhB(MesIm)_3FeNPR_1R_2R_3]$. Our calculations correctly reproduce the experimentally reported decrease in the $T_{1/2}$ with an increasing size of the phosphine, and allow for the prediction of the $T_{1/2}$ in new members of the family that are not reported so far. More importantly, further insight into the factors that control the fine-tuning of the $T_{1/2}$ can be obtained by direct analysis of the underlying electronic structure in terms of the relevant molecular orbitals.

1. Introduction

Spin-Crossover (SCO) molecules are transition metal coordination compounds in which the metal has more than one accessible spin-state.[1] This behavior, reported for the first time by Cambi and coworkers in 1931,[2] and theoretically described by Orgel few years later on the basis of ligand field theory,[3] makes those systems the focus of intense research in physical and chemical sciences due to their inherent technological applications as molecular level switches.[4-9] When a transition metal ion is placed in a given ligand field, if the right combination of coordination number, oxidation state and ligand nature is achieved, the ligand field splitting of the metal center may lead to a situation in which two electronic states are similar in electronic energy. In that case, entropy favors the high-spin state, and spin-crossover may appear, with the low-spin state being observed at low-temperature, and the high-spin state at high temperature.[1] Although thermal spin-crossover is by far the most studied case, other external stimuli such as pressure or electromagnetic radiation may also induce the spin transition.[10-12] The change in the spin-state introduces major changes in the physical properties of the molecule, such as changes in the magnetic moment of the coordination compound, increasing bond-lengths due to the occupation of antibonding orbitals, or color change (changes in the UV-Vis spectrum). As a result of this molecular level switch behavior, SCO systems are ideal candidates for molecular level devices in memory storage systems, particularly due to the possibility of using them in actual devices working at room temperature.[13-15] More recently, the development of Metal-Organic Frameworks (MOFs) that incorporate SCO molecules as secondary building units has lead to the development of the so-called Spin-Crossover Frameworks (SCOFs), which, in many cases, display sensitivity with

respect to the guest nature and loading, thus making these materials perfect candidates for molecular level sensing applications. [12,16-23]

Although SCO was first reported experimentally for pentacoordinated Fe^{III} compounds,[2] over the years it expanded to other coordination numbers and metals in different oxidation state, becoming the most prominent family the hexacoordinated Fe^{II} in octahedral coordination environment.[1,5,9,10,24] Because of its smaller ligand-field splitting, spin-crossover compounds in tetracoordinated transition metal complexes are relatively uncommon, but some examples have been reported and well characterized from the structural and spectroscopic point of view.[25-29] Among these compounds, the recently reported Fe^{II} complexes of general formula $[PhB(MesIm)_3FeNPR_1R_2R_3]$ provides with an interesting family of compounds exhibiting spin-crossover, in which the physical properties can be fine tuned by functionalization of the $\{NPR_1R_2R_3\}^-$ ligand.[26] These compounds offer the possibility of study in detail the subtle effects that ligand functionalization has over the electronic structure of the metal center, thus leading to sensitive changes in the spin-crossover behavior of the molecule. A rational understanding of these effects will help in the design of new spin-crossover molecules with tailored properties.

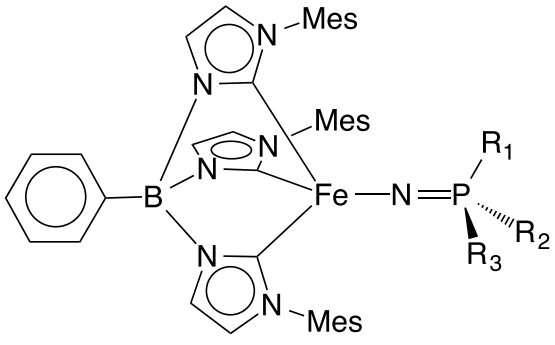

Scheme 1: Schematic of the $[PhB(MesIm)_3FeNPR_1R_2R_3]$ molecule (Mes = 1,3,5-trimethylbenzene)

In this work, we report our theoretical investigation of the [PhB(MesIm)$_3$FeNPR$_1$R$_2$R$_3$] family of compounds using Density Functional Theory (DFT) calculations. Our results show that is possible to compute the transition temperature ($T_{1/2}$), a key parameter in the physical characterization of SCO compound defined as the temperature with equal populations of both spin-states, using first principle tools, which leads to the possible *in silico* design of new species exhibiting spin-crossover. At this point, it is worth to remark that the calculation of transition temperatures in spin-crossover systems is actually pretty challenging for any computational method, due to the fact that it involves the calculation of entropic terms, extremely sensitive to tiny differences in small vibrational frequencies, for both spin states. The results from our calculation allow for a rational understanding of the experimentally reported trend in the change of the $T_{1/2}$ with the phosphine size based on the underlying electronic structure of the metal center in terms of the relevant molecular orbitals involved. Understanding the interplay between the different effects that tune the ligand field of the Fe^{II} metal center is key in the proper design of new SCO molecules with specific transition temperatures. The article is organized as follows: In section 2, the computational methodology is described, while the results are discussed in section 3. Discussion of the results is presented in section 4, and finally the conclusions are outlined in section 5.

2. Methodology

2.1 Computational Details

All Density Functional Theory (DFT) calculations were carried out with Gaussian 09 (revision D.01)[30] electronic structure package with a 10^{-8} convergence

criterion for the density matrix elements, using the hybrid-meta GGA functional TPSSh.[31,32] This functional has been previously used with success in the modeling of accurate thermochemical quantities for several mononuclear Fe^{II} spin-crossover systems.[33,34] The fully optimized contracted triple-ζ all electron Gaussian basis set developed by Ahlrichs and co-workers was employed for all the elements with polarization functions being added on the Fe center.[35] The studied systems have been fully optimized in both spin states (see SI for optimized structures) and subsequently, the vibrational analysis was performed. These results can later be used to compute thermochemical quantities, particularly the temperature dependence of the free energy change, from which one can extract relative populations for each spin-state (see SI for methodological details).[33,34,36] By fitting the ΔG vs. T data, one can extract the corresponding transition temperatures ($T_{1/2}$) for each caclulated system. All the fitting parameters together with the corresponding correlation coefficient can be found in the SI.

3. Results

A total of eight members of the [$PhB(MesIm)_3FeNPR_1R_2R_3$] family have been investigated (Table 1). For each one of these systems, the temperature dependence of the free energy (ΔG) against the temperature was calculated using our previously reported methodology,[33] which allows the calculation of the corresponding transition temperatures ($T_{1/2}$) for each molecule by linear fitting of the ΔG against the temperature (Table 1, SI).

[$PR_1R_2R_3$]	R_1	R_2	R_3	$T_{1/2}$/K
PH_3	-H	-H	-H	378
PMe_3	$-CH_3$	$-CH_3$	$-CH_3$	338(340)
PMe_2nPr	$-CH_3$	$-CH_3$	$-CH_2CH_2CH_3$	257
PMe_2Ph	$-CH_3$	$-CH_3$	$-C_6H_5$	184(271)
PEt_2Me	$-CH_2CH_3$	$-CH_2CH_3$	$-CH_3$	233
$PnPr_3$	$-CH_2CH_2CH_3$	$-CH_2CH_2CH_3$	$-CH_2CH_2CH_3$	185(214)
$PMePh_2$	$-CH_3$	$-C_6H_5$	$-C_6H_5$	136(174)
PPh_3	$-C_6H_5$	$-C_6H_5$	$-C_6H_5$	61(81)

Table 1: Collection of functionalized phosphines used in the [$PhB(MesIm)_3FeNPR_1R_2R_3$] molecules. DFT calculated $T_{1/2}$ values (in K, experimental values for the transition temperatures between parentheses).[26]

The first remarkable feature from the results presented in Table 1 is the good agreement between experimentally reported[26] and calculated transition temperatures. The mean average error is only 28 K (approximately 0.06 kcal/mol), in agreement with previously reported calculations using the TPSSh functional on other SCO molecules.[33] Moreover, the experimental trend is also reproduced, this is, bulkier phosphines lead to smaller transition temperatures. In order to gain further insight into this correlation, we calculated some other members of the [$PhB(MesIm)_3FeNPR_1R_2R_3$] family not yet reported. For all the studied systems, we correlated the computed transition temperature against the Tolman cone angle (θ) and the [He_8] steric parameters.[37-39] The Tolman cone angle, defined as the solid angle formed with the metal at the vertex and the hydrogen atoms at the perimeter of the cone was used in the experimental work to correlate the phosphine size with the shift in the $T_{1/2}$.[26] Given the importance that phosphines have in chemistry, more

sophisticated chemical descriptors have been proposed to improve the quantification of the phosphine size, such as the [He_8] steric parameter. This parameter is defined as the interaction energy between the phosphine in the ground-state conformation and a ring of 8 He atoms, a magnitude that increases with the phosphine size.[37] Both indexes can be correlated with the steric size of the phosphine (Table 2, Figure 1)

[$PR_1R_2R_3$]	θ	[He_8]	$T_{1/2}$
PH_3	87	2.30	378
PMe_3	118	3.00	338(340)
PMe_2*n*Pr	118	3.87	257
PMe_2Ph	122	3.23	184(271)
PEt_2Me	127	4.31	233
P*n*Pr_3	132	6.10	185(214)
$PMePh_2$	136	4.83	136(174)
PPh_3	145	8.00	61(81)

Table 2: DFT computed transition temperatures (in K) for all the [$PhB(MesIm)_3FeNPR_1R_2R_3$] molecules (in parenthesis, experimental values, referència 26???) and the corresponding Tolman cone angle (in degrees) and [He_8] steric parameters.

Juntas Tablas 1 y 2???? Es lo mismo más las dos columnas de los parámetros estéricos

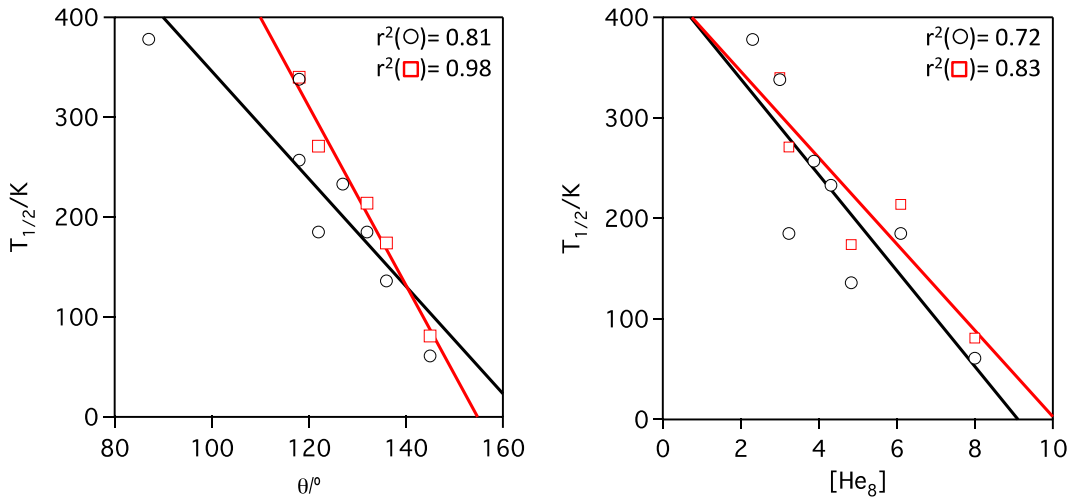

Figure 1: Linear fit of the DFT computed transition (empty circles) temperatures for the [PhB(MesIm)$_3$FeNPR$_1$R$_2$R$_3$] molecules against the Tolman cone angle (left) and [He$_8$] steric (right) parameters. Black (empty circles) for the computed values and red for the experimental data (empty squares).

As can be observed from Figure 1, regardless of the parameter used to quantify the phosphine steric congestion, a decreasing trend in the transition temperature with the phosphine volume is observed. When comparing with the experimental data for the [PhB(MesIm)$_3$FeNPR$_1$R$_2$R$_3$] molecules, a good agreement is achieved, with a slighter better agreement for the [He$_8$] sterics parameter, but in both cases the experimental decrease of the T$_{1/2}$ with larger phosphines is properly reproduced.

An important point that validates the concept of steric control from the phosphine substituents over the SCO transition temperature is the fact that we fully modeled the [PhB(MesIm)$_3$FeNPMe$_3$] molecule as [HB(PhIm)$_3$FeNPMe$_3$], replacing the mesityl groups by phenyl rings. These changes significantly reduce the steric congestion around the PMe$_3$ group, and largely reduce the electronic energy

difference between high- and low-spin states (6.28 and 3.14 kcal/mol respectively). This translates in notable differences in the computed transition temperature, with values for the [PhB(MesIm)$_3$FeNPMe$_3$] and [HB(PhIm)$_3$FeNPMe$_3$] molecules of 338 K and 201 K respectively. Therefore, all calculations require the PhB(MesIm)$_3$ ligand to remain complete, in order to properly model the steric interactions that ultimately lead to the experimentally observed differences in the SCO behavior for the [PhB(MesIm)$_3$FeNPR$_1$R$_2$R$_3$] family. An even more drastic effect can be observed by modeling the mesityl groups by hydrogen atoms. Calculations on the [PhB(Im)$_3$FeNPMe$_3$] and [PhB(Im)$_3$FeNPPh$_3$] systems, provide with computed transition temperatures of 1001 K and 1089 K respectively, which are not only significantly off when compared with the experimental values, but also much more similar between them, as opposite as the observed effect when the complete PhB(MesIm)$_3$ ligand is used. These results strongly support the idea of the ligand fine-tuning control via steric effects of the transition temperature

4. Discussion

Before analyzing the role of the phosphine substituents over the transition temperature, we will briefly discuss the electronic structure of the [PhB(MesIm)$_3$FeNPMe$_3$] and [PhB(MesIm)$_3$FeNPPh$_3$] systems. This is of particular interest due to the fact that very few tetracoordinated spin-crossover molecules have been reported,[24-26,40,41] and characterization of the ligand field effects that lead to the presence of two alternative accessible spin-states is key for the characterization of these systems. In general, due to symmetry considerations, one should expect that the

ligand-field splitting of the d-based molecular orbitals for a tetracoordinated transition metal complex should be small enough so the high-spin situation is always favorable. Notable examples of this situation include the $[Mn(CN)_4]^{2-}$ anion, with four cyanide strong-field ligands, and a magnetic moment of 4.82μ_B, only compatible with an S = 5/2 spin state.[42] This is mostly due to the fact that both sets of orbitals in the tetrahedral ligand field splitting, e and t_2, have a strong antibonding character (Figure 3pones antes la referència a la fig. 3 que a la 2???, yo creo que te refieres la 2), thus leading to a small energy gap between them.

Yo cortaría el párrafo por aquí que es larguísimo y pondria la figura 2

However, for the general case of tetracoordinated $[PhB(MesIm)_3FeNPR_1R_2R_3]$ systems with C_3N coordination sphere, two additional factors are at play. First, the $\{PhB(MesIm)_3\}^-$ ligand introduces a strong umbrella folding distortion on the coordination sphere around the Fe^{II} metal center, which leads to a C_{3v} symmetry point group. In fact, average C-Fe-N angles have been measured from the crystallographic available data on some of the calculated systems, providing with an average value of 127.13º, significantly distant from the 109.47º ideal value for a perfect tetrahedron. This molecular "folding" generates a splitting of the d-based molecular orbitals that, while decreasing the antibonding character on the d_{xy} and d_{x2-y2} orbitals, increases the antibonding character of the d_{xz} and d_{yz} orbitals, therefore increasing the energy gap between the now formally "non-bonding" orbitals and the antibonding orbitals 3). Second, the $\{NPR_1R_2R_3\}^-$ ligand increases the antibonding character of the d_{xz} and d_{yz} orbitals via π-antibonding interactions with the pair of orbitals (Figure 2). The net effect is a resulting ligand field around the metal center that resembles the "3+2" scheme of the octahedral coordination, which effectively generates a splitting among the different subsets of d-based molecular orbitals that provides with the right energy

window for spin-crossover to occur. The effect of such type distortions over the classical tetrahedral orbital splitting have been previously described DFT calculations for tetrahedral cobalt complexes with tripodal phosphine ligands that enforce C_{3v} symmetry.[27]

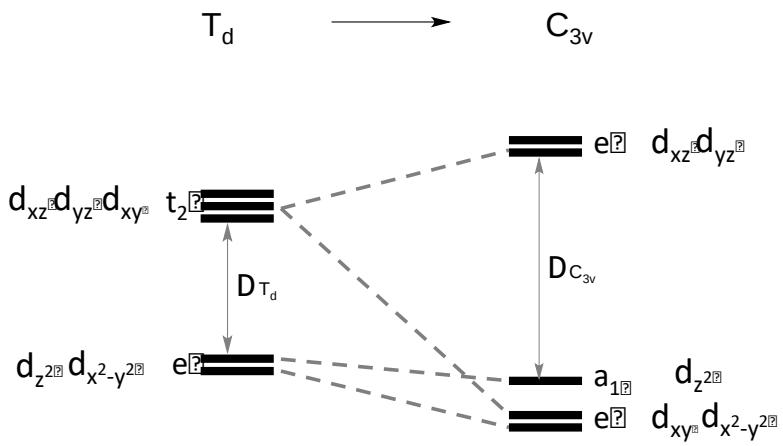

Figure 2: Energy ordering of the d-block molecular orbitals for the [PhB(MesIm)$_3$FeNPR$_1$R$_2$R$_3$] systems in a tetrahedral (T_d, left) and folded umbrella (C_{3v}, right) geometries.

This effect can be corroborated by taking a close inspection to the relevant d-based molecular orbitals for any of the members of the [PhB(MesIm)$_3$FeNPR$_1$R$_2$R$_3$] systems. As an example, in figure 3 we plotted the d-based molecular orbitals for the [PhB(MesIm)$_3$FeNPMe$_3$], which shows the decrease in antibonding character of the d_{xy}, d_{x2-y2} and d_{z2}, with respect to the perfect tetrahedron, thus increasing its non-bonding character, while the d_{yz} and d_{xz} orbital remain strongly antibonding. Similar

patterns are observed for the remaining members of the [PhB(MesIm)$_3$FeNPR$_1$R$_2$R$_3$] family.

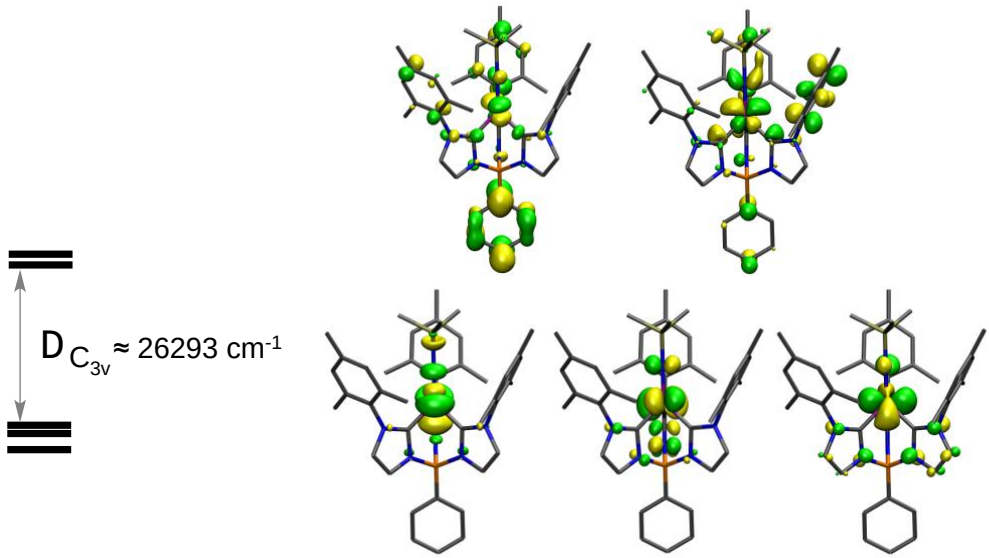

Figure 3: Molecular Orbital diagram for the [PhB(MesIm)$_3$FeNPPh$_3$] (S = 0) molecule, displaying the relevant d-based MOs (isocontour isosurface?? 0.05 e/A$_3$). Hydrogen atoms omitted for clarity. Color scheme: Fe (purple), C (grey), B (orange) and P (yellow). Indicar que la diferencia de energia y los orbitals con los calculados con TPSSh.

At this point, it is interesting (worth) to dive further in the particular set of orbital effects that lead to spin-crossover to appear in this family of compounds. First, and most important, the NPR$_1$R$_2$R$_3$ is key in generating the antibonding interactions that raise the energy of the d_{yz} and d_{xz} orbitals. This can be easy verified by comparing the molecules [PhB(MesIm)$_3$FeNPMe$_3$] and [PhB(MesIm)$_3$FePMe$_3$]$^+$. The second system lacks the N atom, responsible of establishing the antibonding interactions, thus leading to a d-based MO splitting in which the gap among the

orbitals is reduced to Δ_{C3V} = 20598 cm^{-1}, a 22% reduction with respect to the computed gap for the [PhB(MesIm)$_3$FeNPMe$_3$] (Δ_{C3V} = 26293 cm^{-1}). As before, the [PhB(MesIm)$_3$FePMe$_3$]$^+$ exhibits a marked umbrella distortion (average C-Fe-P angle of 124.78 °), responsible for the 3+2 splitting of the d-based MOs (figure 2), but the lack of antibonding character introduced by the N atom leads to a smaller energy gap among them, thus favoring the high-spin over the low-spin state (ΔE_{elec}(HS-LS) = -14.57 kcal/mol), which effectively removes the spin-crossover behavior on the molecule.

A more subtle effect on the antibonding character of the the d_{yz} and d_{xz} pair of orbitals is observed with respect to the antibonding interactions with the C atoms of the {PhB(MesIm)$_3$}$^-$ ligand. In principle, smaller phosphines should allow the Fe atom to get closer to the {PhB(MesIm)$_3$}$^-$ ligand, thus leading to shorter Fe-C bond lengths, which in turn increase the antibonding character of the d_{yz} and d_{xz} orbitals. Such to be the case, smaller phosphines should lead to larger transition temperatures, and the bulkier the phosphine, the smaller the $T_{1/2}$. This can be easily visualized by plotting the $T_{1/2}$ (both computed and experimental) against the average Fe-C bond length (Figure 4a). As can be seen from the plot, a decreasing trend of the $T_{1/2}$ with the Fe-C bond length can be observed, thus proving the phosphine size tuning effect over the spin-crossover transition temperature. Although the slope of the fitting is significantly different between the experimental and the computed data, one must be careful because the experimental bond lengths and angles are subject to crystal packing effects, thus some differences can be expected. The geometrical information for the [PhB(MesIm)$_3$FeNPR$_1$R$_2$R$_3$] is summarized in Table 3.

La primera columna vuelve a salir por tercera vez en una Tabla, mejor juntar las tablas 1 y 2…….

[$PR_1R_2R_3$]	$T_{1/2}$	d(Fe-C)	d(N-P)	d(Fe-N)	C-Fe-N
PH_3	378	1.888	1.683	1.747	126.745
PMe_3	338 (340)	1.892 (1.867)	1.678 (1.556)	1.747 (1.754)	127.02 (127.87)
$PMe_2{}^nPr$	257	1.899	1.682	1.752	126.933
PMe_2Ph	184 (271)	1.898 (1.869)	1.679 (1.541)	1.756 (1.769)	126.99 (127.51)
PEt_2Me	233	1.893	1.685	1.743	127.014
$P{}^nPr_3$	185 (214)	1.903 (1.887)	1.690 (1.571)	1.690 (1.768)	126.95 (127.41)
$PMePh_2$	136 (174)	1.903 (1.882)	1.683 (1.543)	1.760 (1.771)	126.97 (127.34)
PPh_3	61 (81)	1.908 (1.948)	1.686 (1.549)	1.764 (1.807)	126.98 (127.10)

Table 3: Geometric relevant parameters (distances in Å and angles in degrees) for the [$PhB(MesIm)_3FeNPR_1R_2R_3$] molecules and the corresponding DFT calculated transition temperatures (in K). Experimental values provided in parentheses when available. Referencias, 26??? Fe-C bond length and C-Fe-N angle values correspond to the average value.

To further study this effect, a partial optimization scan for the [$PhB(MesIm)_3FeNPMe_3$] molecule using the Fe-B distance as a reaction coordinate has been done. In figure 4b, the difference of electronic energy between high-spin and low-spin states (ΔE_{elec}(HS-LS)) vs. the average Fe-C distance for the computed

structures is depicted. As can be observed, the further the phosphine moves away, reducing the antibonding interaction of the {PhB(MesIm)$_3$}$^-$ ligand with the d_{yz} and d_{xz} MOs, the more stable the high-spin becomes, to the point that crossover takes place around 1.92 Å. Therefore, increasing bond-lengths lead to a progressive stabilization of the high-spin state via reduction of the antibonding interaction with the Fe d_{yz} and d_{xz} d-based MOs, and the high-spin becomes the ground state around 1.92 Å for the average Fe-C bond length, thus indicating a strong effect of the position of the phosphine with respect to the SCO behavior.

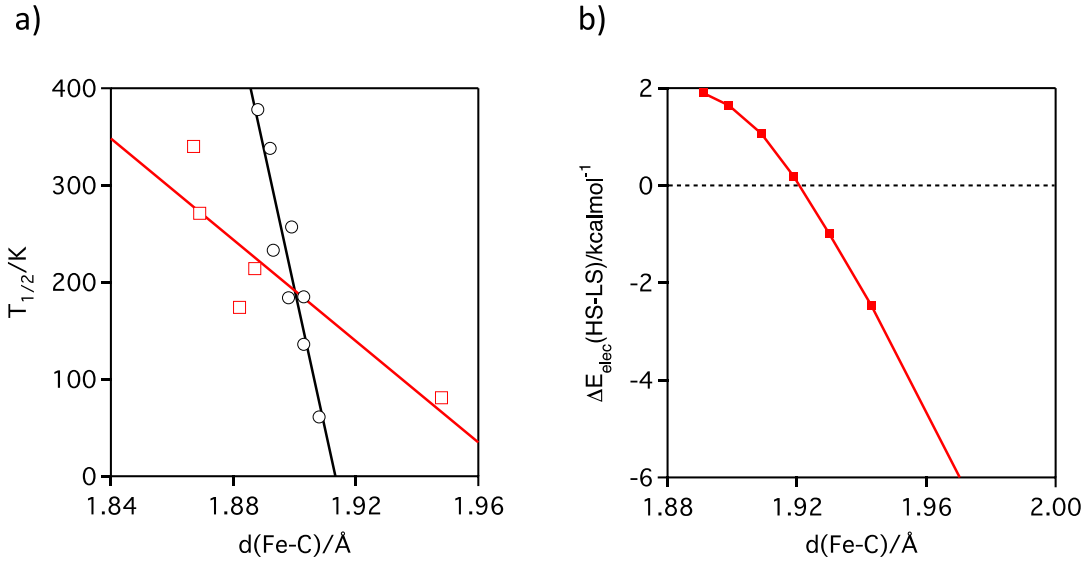

Figure 4: a) Correlation between the average Fe-C bond length and the $T_{1/2}$ (DFT computed in black, experimental in red). b) Relative energies between the high-spin and low-spin states as a function of the average Fe-C bond length.

Finally, it is worth discussing the possibility of modeling electronic effects for isosteric complexes, as reported by Smith and co-workers in the original work for the [PhB(MesIm)$_3$FeNP(*p*-X-C$_6$H$_4$)$_3$] (X = H, Me, OMe) family.[26] This compounds exhibit and increasing shift in the $T_{1/2}$ associated with the donor strength of the *para*-substituent, and effect that can be correlated with the Hammett parameter (σ_p).[43-45]

The calculations correctly reproduce the experimentally observed trend (figure 5), although they are off by around 70 K, due to limitations on the reported computational methodology and the fact that the experimental data was collected in dilute THF solutions. In any case, the calculations shown that electron donating groups increase the energy of the d_{yz} and d_{xz} pair of antibonding orbitals, which in turn increases the energy gap among the d-based MOs. This effect leads to a situation that stabilizes the low-spin state, thus requesting more energy (i.e., higher temperatures) to undergo the spin-transition.

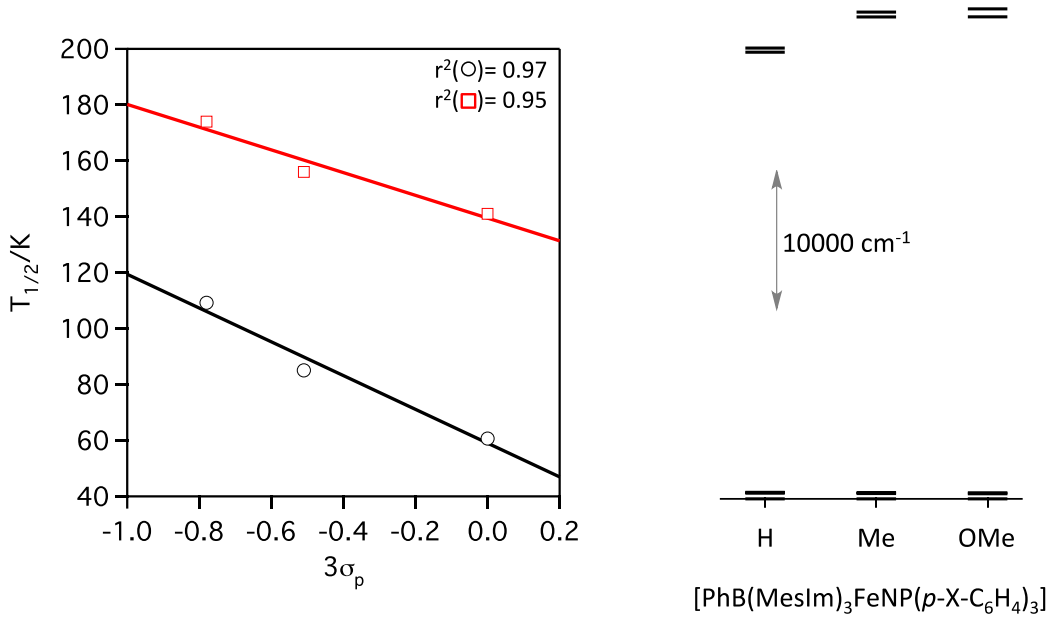

Figure 5: Experimental (red squares) vs. DFT computed (black circles) $T_{1/2}$ for the [PhB(MesIm)$_3$FeNP(*p*-X-C$_6$H$_4$)$_3$] (X = H, Me, OMe) compounds. Right, schematic of the relevant d-based MOs for the low-spin state for the calculated system.

5. Conclusions

In this work we presented our results for the theoretical calculation of the transition temperature ($T_{1/2}$) in tetracoordinated Fe^{II} transition metal complexes of the [PhB(MesIm)$_3$FeNPR$_1$R$_2$R$_3$] family. Using the TPSSh functional, we have shown that it is possible to correctly model the experimental behavior towards spin-crossover displayed by the different members of this family of compounds (i.e, larger

phosphines leading to smaller $T_{1/2}$).[26] The reported calculations correctly model the $T_{1/2}$ dependence with the phosphine size, and allow for the inclusion of previously non-reported members of this family such as [PhB(MesIm)$_3$FeNPH$_3$], [PhB(MesIm)$_3$FeNPMe$_2$*n*Pr] or [PhB(MesIm)$_3$FeNPEt$_2$Me], which correctly fit within the experimentally reported trend, thus proving the potential use of this computational methodology for *in silico* rational ?design of spin-crossover molecules.

As stated above, a clear empirical correlation between the size of the phosphine, either by using the Tolman cone angle or the [He$_8$] steric parameters, [37,39] and the value of the transition temperature can be outlined both, from experimental and computational results. However, we can use the computational results to gain further insight into the factors that govern the fine-tuning control over the spin-crossover properties exhibited by this family of molecules. Spin-crossover is unusual among tetracoordinated transition metal complexes, due to the fact that the splitting among the d-based MOs is usually small when compared to the octahedral case, thus leading to a situation in which the high-spin state is the most favorable situation. However, in the [PhB(MesIm)$_3$FeNPR$_1$R$_2$R$_3$] family, the interplay of three different factors leads to an electronic structure that not only allow for spin-crossover to occur, but also for a very precise tuning of its properties. First, the {PhB(MesIm)$_3$}- ligand introduces a severe umbrella distortion,[46] which decreases the antibonding character of the d_{xy}, d_{x2-y2} and d_{z2} orbitals, thus stabilizing them with respect to the perfect tetrahedron, while the d_{yz} and d_{xz} orbital remain strongly antibonding. However, the distortion itself is not enough to introduce spin-crossover properties in these compounds. For instance, the closely related compound [(tpe)Fe(PMe$_3$)][Li(THF)$_4$] (tpe = tris(5-mesitylpyrrolyl)ethane), also with a strong umbrella distortion (average N-Fe-N angle of 122.00º) remains as an Fe^{II} high spin state, although for this

compound, the tripodal ligand is a much less strong donor.[47] Therefore, the strong antibonding interaction with both the {$NPR_1R_2R_3$}- and the {$PhB(MesIm)_3$}- ligands are key in increasing the antibonding character of the d_{yz} and d_{xz} orbitals, thus leading to a ligand field splitting where the two-spin states have similar electronic energies. The second effect is the π antibonding interaction of the N atom of the {$NPR_1R_2R_3$}- ligand with the d_{yz} and d_{xz} d-based MOs. We have shown that when this interaction is suppressed, for instance modeling the {$NPMe_3$}- as PMe_3, the ligand field gets reduced by a 22%, and the high-spin state becomes the ground state, thus suppressing the SCO behavior. The third factor is the phosphine size, effect that is at play in modulating the antibonding interactions of the C donor atoms of the {$PhB(MesIm)_3$}- ligand towards the d_{yz} and d_{xz} orbitals. Smaller phosphines (i.,e PH_3) allow the Fe^{II} metal center to get closer to the {$PhB(MesIm)_3$}- ligand, thus increasing the destabilization of the d_{yz} and d_{xz} orbitals, while larger phosphine (i.,e PPh_3), blocked by steric hindrance, pull out the Fe^{II} metal center, thus increasing the Fe-C metal-ligand bond lengths, which causes a decrease in the antibonding character of these pair of orbitals, thus reducing the corresponding ligand field splitting. This reduction of the ligand field means, effectively, that the high-spin and low-spin electronic energies become closer, thus requiring less thermal energy (i.e, lower $T_{1/2}$) for the spin-transition to occur. It is worth mentioning that subtle electronic effects induced by electron donating groups in isosteric phosphines can also be properly modeled, although a systematic shift is observed when compared with the experimentally reported data.

To summarize, we have shown how the use of computational tools can provide with further insight in the experimental behavior of the [$PhB(MesIm)_3FeNPR_1R_2R_3$] family of compounds displaying spin-crossover, not

only by correctly reproducing the experimental behavior, but also by providing with the mechanisms that control the electronic structure of these systems and control the spin-crossover behavior. The good agreement between experimental data and computed values for the $T_{1/2}$, together with the inclusion of experimentally non-reported members of these family validate the presented computational methodology as a powerful tool in the computationally assisted design of coordination compounds exhibiting spin-crossover properties.

Associated Content

Cartesian atomic coordinates for the [$PhB(MesIm)_3FeNPR_1R_2R_3$] optimized geometries and fitting parameters for the thermochemical quantities (ΔH, ΔG and $T\Delta S$) as a function of the temperature for each studied system. This material is available free of charge at http://pubs.acs.org

Author information

jordi.cirera@qi.ub.es

eliseo.ruiz@qi.ub.es

Notes: The authors declare no competing financial interest.

Acknowledgments

J.C. gratefully acknowledges financial support from the Generalitat de Catalunya (7_{th} program Beatriu de Pinos-Marie Curie co-fund Fellowship, 2013 BP-B 00155). E.R. thanks Generalitat de Catalunya for an ICREA Academia fellowship. We thank *Consorci de Serveis Universitaris de Catalunya* (CSUC) for computational Resources.

References:

(1) *Spin Crossover in Transition Metal Compounds* Gütlich, P.; Goodwin, H. A., Eds.; Springer: New York, 2004; Vol. 233-235.
(2) Cambi, L.; Szego, L. *Ber. Dtsch. Chem. Ges.* **1931**, *64*, 2591-2598.
(3) Griffith, J. S.; Orgel, L. E. *Q. Rev. Chem. Soc.* **1957**, *11*, 381-393.
(4) Bousseksou, A.; Molnar, G.; Salmon, L.; Nicolazzi, W. *Chem. Soc. Rev.* **2011**, *40*, 3313-3335.
(5) Goodwin, H. A. *Coord. Chem. Rev.* **1976**, *18*, 293-325.
(6) Gütlich, P. *Struct. Bond.* **1981**, *44*, 83-195.
(7) König, E. *Struct. Bond.* **1991**, *76*, 51-152.
(8) Nihei, M.; Shiga, T.; Maeda, Y.; Oshio, H. *Coord. Chem. Rev.* **2007**, *251*, 2606-2621.
(9) Toftlund, H. *Coord. Chem. Rev.* **1989**, *94*, 67-108.
(10) Gütlich, P.; Garcia, Y.; Goodwin, H. A. *Chem. Soc. Rev.* **2000**, *29*, 419-427.
(11) Real, J. A.; Gaspar, A. B.; Munoz, M. C. *Dalton Trans.* **2005**, 2062-2079.
(12) Thompson, A. L.; Money, V. A.; Goeta, A. E.; Howard, J. A. K. *C. R. Chim.* **2005**, *8*, 1365-1373.
(13) Bousseksou, A.; Molnar, G.; Matouzenko, G. *Eur. J. Inorg. Chem.* **2004**, 4353-4369.
(14) Kahn, O.; Martinez, C. J. *Science* **1998**, *279*, 44-48.
(15) Salitros, I.; Madhu, N. T.; Boca, R.; Pavlik, J.; Ruben, M. *Monatsh. Chem.* **2009**, *140*, 695-733.
(16) Muñoz, M. C.; Real, J. A. *Coord. Chem. Rev.* **2011**, *255*, 2068-2093.
(17) Cirera, J. *Rev. Inorg. Chem.* **2014**, *34*, 199-216.
(18) *Spin-Crossover Materials: Properties and Applications*; Halcrow, M. A., Ed.; John Wiley & Sons: Hoboken, 2013.
(19) Halder, G. J.; Chapman, K. W.; Neville, S. M.; Moubaraki, B.; Murray, K. S.; Letard, J.-F.; Kepert, C. J. *J. Am. Chem. Soc.* **2008**, *130*, 17552-17562.
(20) Halder, G. J.; Kepert, C. J.; Moubaraki, B.; Murray, K. S.; Cashion, J. D. *Science* **2002**, *298*, 1762-1765.
(21) Neville, S. M.; Halder, G. J.; Chapman, K. W.; Duriska, M. B.; Moubaraki, B.; Murray, K. S.; Kepert, C. J. *J. Am. Chem. Soc.* **2009**, *131*, 12106-+.
(22) Neville, S. M.; Halder, G. J.; Chapman, K. W.; Duriska, M. B.; Southon, P. D.; Cashion, J. D.; Letard, J.-F.; Moubaraki, B.; Murray, K. S.; Kepert, C. J. *J. Am. Chem. Soc.* **2008**, *130*, 2869-2876.
(23) Neville, S. M.; Moubaraki, B.; Murray, K. S.; Kepert, C. J. *Angew. Chem. Int. Ed.* **2007**, *46*, 2059-2062.

(24) Thuery, P.; Zarembowitch, J. *Inorg. Chem.* **1986**, *25*, 2001-2008.
(25) Bowman, A. C.; Milsmann, C.; Bill, E.; Turner, Z. R.; Lobkovsky, E.; DeBeer, S.; Wieghardt, K.; Chirik, P. J. *J. Am. Chem. Soc.* **2011**, *133*, 17353-17369.
(26) Lin, H.-J.; Siretanu, D.; Dickie, D. A.; Subedi, D.; Scepaniak, J. J.; Mitcov, D.; Clerac, R.; Smith, J. M. *J. Am. Chem. Soc.* **2014**, *136*, 13326-13332.
(27) Jenkins, D. M.; Peters, J. C. *J. Am. Chem. Soc.* **2005**, *127*, 7148-7165.
(28) Min, K. S.; Arthur, J.; Shum, W. W.; Bharathy, M.; zur Loye, H.-C.; Miller, J. S. *Inorg. Chem.* **2009**, *48*, 4593-4594.
(29) Jenkins, D. M.; Peters, J. C. *J. Am. Chem. Soc.* **2003**, *125*, 11162-11163.
(30) falta Gaussian release….. Frisch, M. J.; Trucks, G. W.; Schlegel, H. B.; Scuseria, G. E.; Robb, M. A.; Cheeseman, J. R.; Scalmani, G.; Barone, V.; Mennucci, B.; Petersson, G. A.; Nakatsuji, H.; Caricato, M.; Li, X.; Hratchian, H. P.; Izmaylov, A. F.; Bloino, J.; Zheng, G.; Sonnenberg, J. L.; Hada, M.; Ehara, M.; Toyota, K.; Fukuda, R.; Hasegawa, J.; Ishida, M.; Nakajima, T.; Honda, Y.; Kitao, O.; Nakai, H.; Vreven, T.; Montgomery Jr., J. A.; Peralta, J. E.; Ogliaro, F.; Bearpark, M. J.; Heyd, J.; Brothers, E. N.; Kudin, K. N.; Staroverov, V. N.; Kobayashi, R.; Normand, J.; Raghavachari, K.; Rendell, A. P.; Burant, J. C.; Iyengar, S. S.; Tomasi, J.; Cossi, M.; Rega, N.; Millam, N. J.; Klene, M.; Knox, J. E.; Cross, J. B.; Bakken, V.; Adamo, C.; Jaramillo, J.; Gomperts, R.; Stratmann, R. E.; Yazyev, O.; Austin, A. J.; Cammi, R.; Pomelli, C.; Ochterski, J. W.; Martin, R. L.; Morokuma, K.; Zakrzewski, V. G.; Voth, G. A.; Salvador, P.; Dannenberg, J. J.; Dapprich, S.; Daniels, A. D.; Farkas, Ö.; Foresman, J. B.; Ortiz, J. V.; Cioslowski, J.; Fox, D. J.; Gaussian, Inc.: Wallingford, CT, USA, 2009.
(31) Tao, J. M.; Perdew, J. P.; Staroverov, V. N.; Scuseria, G. E. *Phys. Rev. Lett.* **2003**, *91*.
(32) Staroverov, V. N.; Scuseria, G. E.; Tao, J. M.; Perdew, J. P. *J. Chem. Phys.* **2003**, *119*, 12129-12137.
(33) Cirera, J.; Paesani, F. *Inorg. Chem.* **2012**, *51*, 8194-8201.
(34) Jensen, K. P.; Cirera, J. *J. Phys. Chem. A* **2009**, *113*, 10033-10039.
(35) Schäfer, A.; Huber, C.; Ahlrichs, R. *J. Chem. Phys.* **1994**, *100*, 5829-5835.
(36) Cirera, J.; Ruiz, E. *J. Mater. Chem. C* **2015**, *3*, 7954-7961.
(37) Jover, J.; Fey, N.; Harvey, J. N.; Lloyd-Jones, G. C.; Orpen, A. G.; Owen-Smith, G. J. J.; Murray, P.; Hose, D. R. J.; Osborne, R.; Purdie, M. *Organometallics* **2010**, *29*, 6245-6258.
(38) Müller, T. E.; Mingos, D. M. P. *Transition Met. Chem.* **1995**, *20*, 533-539.
(39) Tolman, C. A. *J. Am. Chem. Soc.* **1970**, *92*, 2956-&.
(40) Kennedy, B. J.; Fallon, G. D.; Gatehouse, B.; Murray, K. S. *Inorg. Chem.* **1984**, *23*, 580-588.
(41) Mossin, S.; Tran, B. L.; Adhikari, D.; Pink, M.; Heinemann, F. W.; Sutter, J.; Szilagyi, R. K.; Meyer, K.; Mindiola, D. J. *J. Am. Chem. Soc.* **2012**, *134*, 13651-13661.
(42) Buschmann, W. E.; Arif, A. M.; Miller, J. S. *Angew. Chem. Int. Ed.* **1998**, *37*, 781-783.
(43) Hammett, L. P. *Chemical Reviews* **1935**, *17*, 125-136.
(44) Hammett, L. P. *J. Am. Chem. Soc.* **1937**, *59*, 96-103.
(45) Hansch, C.; Leo, A.; Taft, R. W. *Chemical Reviews* **1991**, *91*, 165-195.
(46) Cirera, J.; Alemany, P.; Alvarez, S. *Chem. Eur. J.* **2004**, *10*, 190-207.
(47) Sazama, G. T.; Betley, T. A. *Inorg. Chem.* **2014**, *53*, 269-281.

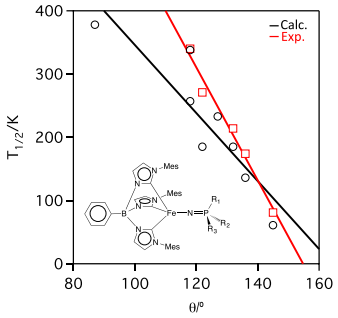

TOC: For Table of Contents Only

Synopsis

A Density Functional Theory (DFT) methodology for quantitative calculation of transition temperature ($T_{1/2}$) in tetracoordinated spin-crossover compounds of general formula [$PhB(MesIm)_3FeNPR_1R_2R_3$] is reported. The method fully agrees with the experimentally reported data and is able to predict the $T_{1/2}$ for new members of the family. Insight into the fine-tuning control over the $T_{1/2}$based on the phosphine size is reported by analysis of the corresponding molecular orbitals.